RESEARCH ARTICLE
doi: 10.2306/scienceasia1513-1874.2026.s001

ScienceAsia 52S (1): 2026: ID 2026s001: **1–13**

Safe removal of aged polyvinyl acetate binder from canvas using nanocellulose aerogel: preserving original color of artworks

Atikarn Kraichok[a], Watsachon Leksomboon[a], Sasia Leelathaweewat[a], Siriyakorn Khumsang[a], Ochana Poonthongdeewatthana[b], Nicole Tse[c], Kamonwan Pacaphol[a,*]

[a] Department of Imaging and Printing Technology, Faculty of Science, Chulalongkorn University, Bangkok 10330 Thailand

[b] Department of Art Theory, Faculty of Painting Sculpture and Graphic Arts, Silpakorn University, Bangkok 10200 Thailand

[c] The Robert Cripps Institute for Cultural Conservation, Faculty of Arts, University of Melbourne, Victoria 3010 Australia

*Corresponding author, e-mail: kamonwan.p@chula.ac.th

Received 29 Dec 2025, Accepted 20 Jul 2026
Available online 30 Sep 2026

ABSTRACT: In artwork remedial conservation, inappropriate cleaning methods can cause undesirable discoloration and irreversible damage to artwork surfaces. Conventional cotton-swab cleaning often poses challenges due to uncontrolled liquid release and inconsistent manual force. To address these issues, soft hydrogels have been developed as cleaning materials. This study developed a hydrogel capable of loading water-based cleaning solutions from bacterial nanocellulose (BNC) and evaluated its effectiveness in removing aged polyvinyl acetate (PVAc), a binder commonly used by Thai artists, from linen canvas. BNC hydrogels were prepared using different drying techniques and subsequently loaded with acetic acid or citric acid solutions at various concentrations. Among all techniques, supercritical CO_2 drying produced a BNC aerogel with the best recovery of hydrogel characteristics and mechanical properties after solution loading. The BNC hydrogel loaded with 10% w/v citric acid achieved the most effective PVAc removal after eight cleaning cycles (80 min total) with suction applied beneath the canvas. The treated canvas exhibited a total color difference (ΔE) of less than 2 compared with the original PVAc-free canvas and showed the lowest residual carbonyl peak of PVAc in FTIR analysis. SEM images further revealed more individualized fibers and a reopened porous structure resembling that of the original canvas. Moreover, the BNC hydrogel retained its mechanical properties after use, indicating its reusability. These findings demonstrate the potential of BNC aerogel as a solution carrier for canvas cleaning, with promising applicability to other types of artwork substrates.

KEYWORDS: bacterial nanocellulose, aerogel, canvas conservation, cleaning gel

INTRODUCTION

In recent years, cleaning techniques have been developed to be more suitable for each type of artwork. Three main types of artwork that have been categorized—painting, sculpture, and architecture—require careful cleaning techniques to prevent damage to their surfaces. One of the main problems in artwork remedial conservation is related to cleaning methods, including the improper use of cleaning techniques, chemicals, and equipment, which can lead to surface damage and deterioration [1]. Conventional cleaning procedures consist of two approaches, mechanical and chemical, which are usually applied together. Improper use of these approaches can cause damage to the artwork's surface. For instance, the mechanical approach that applies excessive rubbing force with cotton swabs or fabric, or the chemical approach that uses overly strong solvents or an excessive amount of solvents, can both result in scratches and swelling on the surface, or the removal of original materials such as pigments and binders from the artwork. Therefore, a porous gel highly-absorbing solution or water called hydrogel was introduced in the 1980s [2]. These gels were designed to improve cleaning efficiency by incorporating cleaning solutions that become absorbed within their highly porous and polar structures [1]. Materials commonly used to produce these gels include polyallylamine, polyacrylamide, poly(ethyl methacrylate), poly(vinyl alcohol) (PVA), and poly(vinyl acetate) (PVAc) [2, 3]. The double-network PVA gels have been shown to improve mechanical stability, reduce water release, and better localization of cleaning agents on oil-painting substrates [2]. However, because these gels are synthetic resins derived from non-renewable resources, they still require the incorporation of various chemical components during production, consequently adding to the carbon footprint and raising concerns regarding environmental sustainability.

Bio-based polymer hydrogels have been increasingly explored as renewable alternatives for developing more sustainable hydrogel systems. A green-algae polysaccharide-based hydrogel was developed using microwave-assisted alkaline extraction followed by free-radical graft copolymerization, resulting in a

porous network with a high swelling ratio [4]. In the context of art conservation, polysaccharide gels such as agarose and gellan gum have been employed to confine aqueous or mildly acidic solutions and reduce solvent penetration into canvas and other porous supports. However, the release of inappropriate amounts of liquid and their poor conformability to textured surfaces have limited their effectiveness in treating aged binder layers [5, 6]. Organogels, in which organic solvents are immobilized within a three-dimensional gel network, were also introduced to deliver organic solvents more selectively for reducing wax-resin and similar coatings on easel paintings, but their rigidity and reliance on solvent-based formulations restricted their broader use in water-based cleaning [1, 7]. In addition, these gel systems often require long contact times to soften aged binders, may still over-wet weakened canvas fibers, and do not always adapt well to the weave structure of textile supports [8, 9]. These limitations indicate that further development is needed to achieve safe and efficient removal of aged binders from canvas surfaces. Recently, cellulose nanocrystal (CNC)- and long-nanofiber-based aerogels and hydrogels have been explored as cellulose-derived materials with high porosity and strong water retention, enabling controlled uptake and release of aqueous media. These systems can be prepared via sol-gel processes combined with drying techniques such as supercritical CO_2 drying. However, the relatively rigid structure of CNC-dominated networks may limit their conformability on uneven or fragile substrates, which can restrict their applicability in delicate conservation cleaning [10, 11]. In this context, long nanofibers are likely to be more suitable for conservation cleaning due to their softer and more flexible network structure, providing a more conformable matrix for contact with sensitive surfaces. These long nanofibers can be obtained from plant sources as cellulose nanofibers (CNF) or produced microbially as bacterial nanocellulose (BNC).

BNC is produced from renewable resources through the cultivation of non-pathogenic bacteria in a glucose-rich culture medium derived from agricultural products. Structurally, BNC is a homopolymer of glucose units linked by β-glycosidic bonds and synthesized by various bacterial genera such as *Acetobacter*, *Agrobacterium*, *Azotobacter*, *Rhizobium*, and *Pseudomonas*, with *Acetobacter xylinum* being the most widely employed [12]. BNC exhibits distinctive characteristics including nanoscale fiber dimensions, high cellulose purity, excellent water-holding capacity, remarkable tensile strength and Young's modulus, and high flexibility, while also offering low production costs, environmental friendliness, and biodegradability [13]. Although BNC shares the same molecular structure as plant-derived cellulose, it differs markedly in morphology, possessing a unique, highly porous three-dimensional network that contributes to its nano-structural gel formation without the use of a crosslinker. Its purity—free of hemicellulose and lignin—along with abundant hydroxyl groups that confer strong hydrophilicity and a crystallinity level of approximately 80–90%, further enhances its performance [14]. Consequently, these characteristics make BNC a promising candidate for use as a cleaning gel to replace the synthetic gels mentioned above, as it meets essential requirements for artwork restoration materials, including high absorption of water-based cleaning solutions, excellent water retention, controlled release, high softness and flexibility combined with strong tensile strength allowing close conformity to rough artwork surfaces and residue-free removal after use, safety for both artworks and conservators, customizable shapes for specific applications, and reasonable production costs [15].

In this work, a highly porous hydrogel derived from BNC was introduced for removing aged binder residues from canvas, a necessary step in the remedial conservation of artworks in which deteriorated binders or priming layers must be eliminated prior to restoration. Because water-based solutions needed to be incorporated into the BNC hydrogel to replace water, different dehydration techniques for preparing the dried BNC matrix were investigated, with slight adaptations from our previous study. Three dehydration methods were employed: dehydration under ambient pressure, freeze-drying, and supercritical CO_2 (SC-CO_2) drying. After drying, mild organic water-based solutions—acetic acid and citric acid at various concentrations—were loaded into the dried BNC pieces and subsequently applied for cleaning aged binder from linen canvas surfaces at different contact times. To simulate deterioration found in real artworks, PVAc, an adhesive and binder widely used by Thai artists, was first applied to the canvas and then artificially aged through an accelerated aging process. To the best of our knowledge, this approach—utilizing BNC hydrogels loaded with water-based solutions for artwork cleaning—represents a novel method proposed by our research group, with the present study focusing specifically on its application for PVAc removal from canvas substrates. To evaluate the effectiveness of this cleaning approach, physical changes using visual inspection, color difference measurements using a colorimeter, chemical structural changes analyzed by Fourier transform infrared spectroscopy (FTIR), and morphological changes observed via scanning electron microscopy (SEM) were examined.

METHODOLOGY

Materials and chemicals

PVAc latex (grade no. LA-22S) was obtained from TOA Paint Thailand, containing approximately 50% PVAc within the total solid content. The raw BNC, cultivated using *A. xylinum* in mature coconut water under static fermentation conditions, was graciously

provided by the Banlangsawat Coconut Jelly Factory in Samut Songkhram, Thailand. The chemicals used for purifying the BNC—sodium lauryl sulfate (SLS), sodium hydroxide (NaOH), and hydrogen peroxide (H_2O_2)—were all analytical reagent (AR) grade and sourced from Chem-Supply Pty Ltd, Australia. AR-grade absolute ethanol was purchased from QRëC, New Zealand. AR-grade acetic acid and citric acid were obtained from RCI Labscan, Thailand, and Loba Chemie, India, respectively.

Preparation of linen canvas

Linen canvas was coated with PVAc latex using a K-control coater (K202 Control Coater, RK Print Coat Instruments, England) equipped with a spirally wound bar No. 150, producing a wet film thickness of approximately 150 µm. After drying at ambient temperature, the coated canvas was baked at 120 °C for 72 h to induce aging, simulating the characteristics of aged canvas fabric following the approach described by Ahmed and Kolisis [16]. The aged canvas was then cut into squares of approximately 5×5 cm and stored in a desiccator.

Preparation of dried BNC for loading cleaning solutions

The raw BNC hydrogel was converted into dried BNC gels using a procedure slightly modified from our previous study [15]. Briefly, the raw hydrogels were cut into pieces measuring 2.5×2.5×0.4 cm and purified by sequentially soaking them in 2% w/v SLS overnight, in 0.5 M NaOH at 80 °C for 1 h, in 1.5% v/v H_2O_2 at room temperature for 30 min, and finally neutralizing them with deionized water. The hydrogel pieces were then subjected to different drying techniques. The first method involved drying under ambient conditions by placing the hydrogels in a closed container filled with silica gel. The second method employed freeze-drying using a freeze dryer (Beta 1–8 LDplus, Martin Christ, Germany) at 0.2 mbar for 48 h. The third method employed supercritical CO_2 drying (EM CPD300 Critical Point Dryer, Leica, Germany) at 38 °C for 130 min, in which the hydrogel samples were subjected to solvent exchange until absolute ethanol completely replaced the water within the gel matrix prior to drying. All dried samples were subsequently stored in a desiccator for further experiments.

Water-based solution loading performance of dried BNC

Three dried BNC samples were designated as xerogel, cryogel, and aerogel, following the drying methods of ambient-condition drying, freeze-drying, and supercritical CO_2 drying, respectively. In this test section, water was employed as a representative water-based cleaning solution and was loaded into the samples through soaking. The water-uptake performance and the water-release behavior on canvas after uptake were examined to determine the optimal drying method for preparing dried BNC sample for the application. The experiments were conducted in triplicate.

The liquid-uptake performance was evaluated by immersing the dried BNC in DI water, 10% v/v acetic acid solution, and 10% w/v citric acid solution at room temperature (approximately 25 ± 2 °C). The weight of the swollen BNC was recorded at 2, 4, 16, and 24 h. The amount of liquid uptake was calculated using an equation adapted from the moisture content study by Kumar et al [17]. The calculation was based on the equation:

$$\text{Liquid uptake (\%)} = \frac{(W - W_{\text{dry}}) \times 100}{(W_0 - W_{\text{dry}})} \qquad (1)$$

where W is the BNC weight after liquid uptake at each time point (g), W_{dry} is the BNC weight after drying (g), and W_0 is the BNC weight before drying (g).

The liquid-release behavior, the fully liquid-loaded BNC and cotton pad (fiber diameter of 16 µm) were placed onto the commercially sized canvas at room temperature. The weight of the canvas was recorded every 20 min for 2 h. The liquid release was calculated based on the increase in canvas weight relative to the weight before testing [15].

Application of BNC hydrogels for removing aged binder from canvas

The selected dried BNC sample was employed to be loaded with two cleaning solutions, namely acetic acid and citric acid, at concentrations of 1%, 5%, and 10% in DI water. The loading was performed by soaking the samples for 4 h to allow complete solution uptake and transformation into hydrogels, as shown in the experimental layout in Fig. 1. Afterward, the hydrogel was placed in close contact with the canvas surface together with a suction force applied underneath the canvas using a vacuum pump (pressure: 20 kPa) for various durations, specifically 2, 4, and 8 cycles (10 min per cycle; the short contact time per cycle was selected to minimize over-wetting, which is particularly important for hydrophilic cellulose-based substrates [18]). In each cycle, hydrogel pieces were re-soaked in the corresponding solution and alternated for use. In this experiment, a water-loaded cotton pad and water-loaded BNC were used as control samples. After treatment, the canvas was neutralized using a water-moistened cotton swab and subsequently stored in a desiccator under ambient conditions to remove moisture prior to characterization.

Characterization and property test

Morphologies of BNC and canvas

The morphologies of the BNC and linen canvas were investigated using a scanning electron microscope (SEM; JSM-6610LV, JEOL, Germany). All samples were dried,

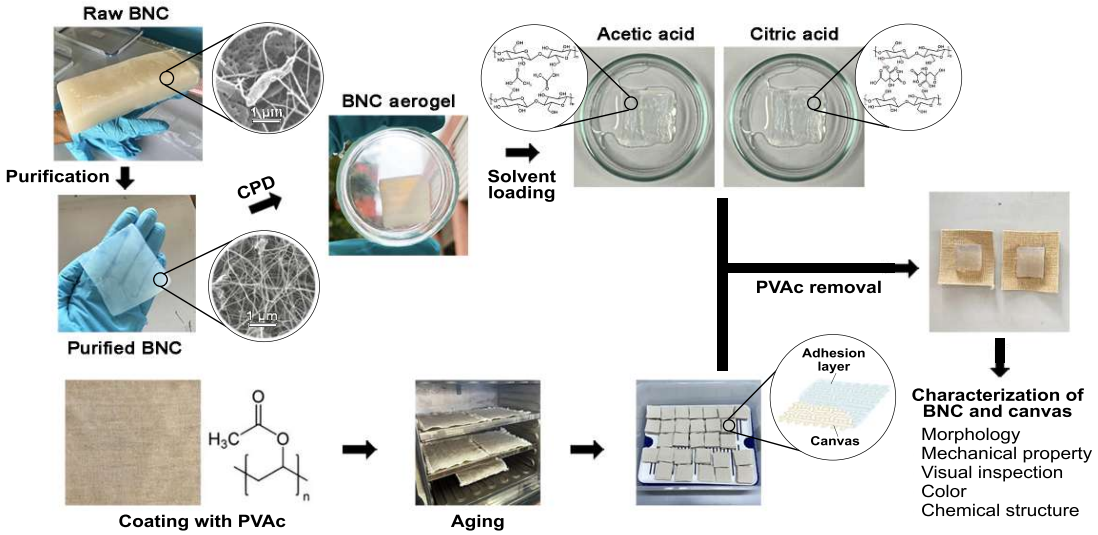

Fig. 1 Experimental diagram of BNC aerogel used for removing PVAc from canvas.

cut into 0.5×0.5 cm pieces, and then gold-sputter coated to ensure electrical conductivity. The morphological analysis was performed at accelerating voltages in the range of 5–10 kV.

Mechanical properties of BNC

The mechanical properties of the hydrogel, including its storage modulus (G′) and loss modulus (G″), were evaluated using a cone-plate rheometer (HAAKE MARS iQ Air, Thermo Fisher Scientific, Germany) equipped with a P20/Ti plate rotor suitable for hydrogel samples. The experiment was performed under controlled conditions at 25 °C with a frequency sweep ranging from 0.1 to 25 Hz.

Color difference of canvas before and after PVAc removal

The canvas samples were photographed in a light box under the CIE standard illuminant D65 and UV light to examine the physical and color change after PVAc removal. In addition, the color values (CIE L*a*b*) of the original canvas without PVAc after aging (aging condition: 120 °C for 72 h) and the canvas after PVAc removal were measured using a colorimeter (CR-400, Konica Minolta, Japan) under the CIE standard illuminant D65 with a 2° observer angle. The color difference value was calculated to investigate the change of surface color.

Chemical structure of canvas before and after PVAc removal

Attenuated Total Reflectance–Fourier Transform Infrared (ATR-FTIR) spectroscopy (Nicolet iS5, Thermo Scientific, Waltham, MA, USA) was used to record spectra of the tested areas before and after PVAc removal. Samples were kept in a silica-gel desiccator at room temperature prior to testing. Spectra were collected in absorbance mode over 400–4000 cm^{-1} with 64 scans at a resolution of 8 cm^{-1}.

Statistical analysis

The statistical analysis was performed using SPSS Statistics version 28 (IBM, Chicago, IL, USA). The data obtained from the experiments were analyzed to determine significant differences among the PVAc removal methods and the cleaning cycles. One-way analysis of variance (ANOVA) was conducted, followed by Duncan's Multiple Range Test at a significance level of $p < 0.05$.

RESULTS AND DISCUSSION

Morphology of BNC

The morphology of the raw (post-fermentation) and purified BNC was examined using photographs and SEM images. The raw BNC, shown in Fig. 2a, exhibits cellulose fibers produced by the bacteria, and remnants of rod-shaped bacterial cells can still be observed (red circle). Residues of the culture medium, together with remaining bacterial debris, are present within the fibrous network, resulting in the cloudy and yellowish appearance of the BNC (Fig. 2c). After purification, the BNC displayed smaller fiber sizes, with fiber diameters of approximately 20–60 nm, and a clear porous network free of bacterial cells (Fig. 2b), where traces of sites previously occupied by bacterial cells can still be discerned. The purified BNC appeared brighter, whiter, and more translucent (Fig. 2d), making it suitable for further development as a cleaning gel. These results confirm that the purification process effectively removes bacterial cells, culture medium residues, and other impurities from the raw BNC.

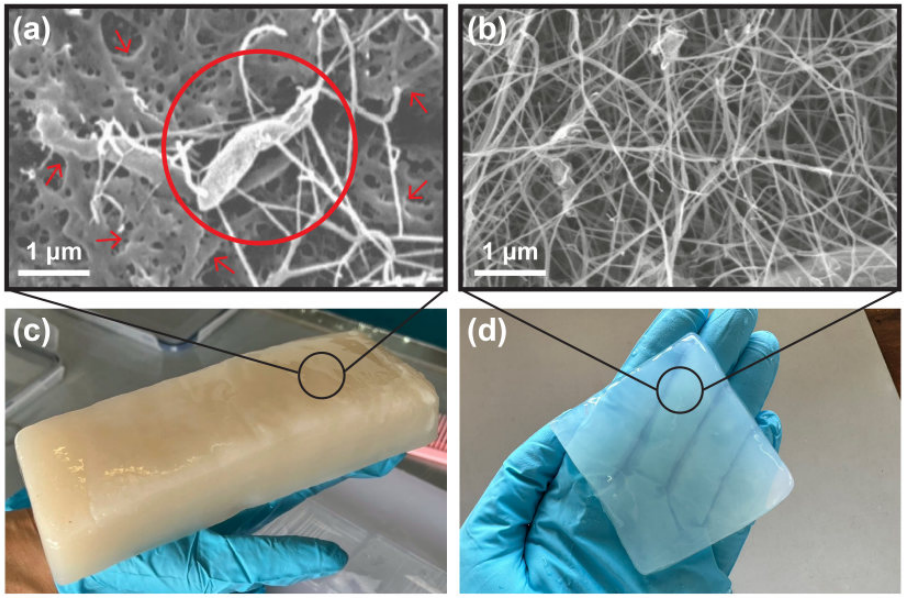

Fig. 2 SEM images (top) and corresponding photographs (bottom) of BNC hydrogels before (left) and after (right) purification. Red circle in (a) indicates a dead rod-shaped bacterial cell, while red arrows indicate residual culture medium.

Liquid uptake of dried BNC and release performance of BNC hydrogel

The physical appearances of dried BNC before and after water uptake are shown in Fig. 3a. In this study, the dried BNC samples obtained using different drying methods were classified as xerogel, cryogel, and aerogel, corresponding to ambient drying, freeze-drying, and supercritical CO_2 drying, respectively. According to our previous work [15], these drying methods produced dried BNC materials with markedly different densities and porosities. The densities of the xerogel, cryogel, and aerogel were 0.16 ± 0.02, 0.018 ± 0.005, and 0.007 ± 0.001 g/cm^3, while their porosities were 2 ± 1, 39 ± 10, and 86 ± 9%, respectively. Among these materials, the BNC prepared by supercritical CO_2 drying can be designated as an aerogel because it exhibited the characteristic features of aerogel materials, which are typically described as highly porous, low-density materials with densities in the range of 0.001–0.1 g/cm^3 and porosities commonly ranging from 80 to 99.8% [19]. According to Fig. 3a, the rehydrated BNC aerogel became more translucent and was able to recover its hydrogel structure. In contrast, both the xerogel and cryogel were unable to regain the original hydrogel dimensions prior to drying. This observation is consistent with the water uptake results presented in Fig. 3b, which illustrate the kinetics of water reabsorption into the BNC network. The xerogel and cryogel exhibited water uptake values of only 3% and 19%, respectively, during the first 2 h, and only slight increases in water uptake over time, implying limited structural recovery. In comparison, the aerogel showed remarkably higher water uptake, reaching approximately 70% within 2 h and gradually increasing to 85% after 24 h of immersion. The density of the dried aerogel increased markedly from 0.007 ± 0.001 g/cm^3 to 1.36 ± 0.26 g/cm^3 after 24 h of water soaking [15], indicating a water content of approximately 99 wt% based on the density change. This high water content is consistent with the definition of a hydrogel as a three-dimensional polymeric network containing more than 90% water, while preserving its gel-like form and water-retaining network [20].

The observed result is mainly due to the ability of supercritical CO_2 drying to retain both the high surface area of nanofibers with abundant hydroxyl groups on their surface and the integrity of the nanoporous network. Since the increase in capillary forces during drying is inhibited by this technique, fiber agglomeration is prevented and nanopore collapse is significantly minimized [21]. In contrast, when the hydrogel was completely dried under uncontrolled ambient conditions (xerogel sample) or by freeze-drying (cryogel sample), the CNF moved into closer contact. This phenomenon caused secondary bonding between adjacent nanofibers, resulting in structural shrinkage. Furthermore, the capillary stress generated during freeze-drying disrupted the nanoporous network, deforming the pore structure and increasing the pore size relative to the original hydrogel [22], thereby restricting the water-uptake capacity of both the xerogel and cryogel samples.

Fig. 3d presents the water-release behavior on canvas of BNC hydrogels rehydrated from the xerogel, cryogel, and aerogel samples, compared with a commercial cotton pad. The xerogel and cryogel samples

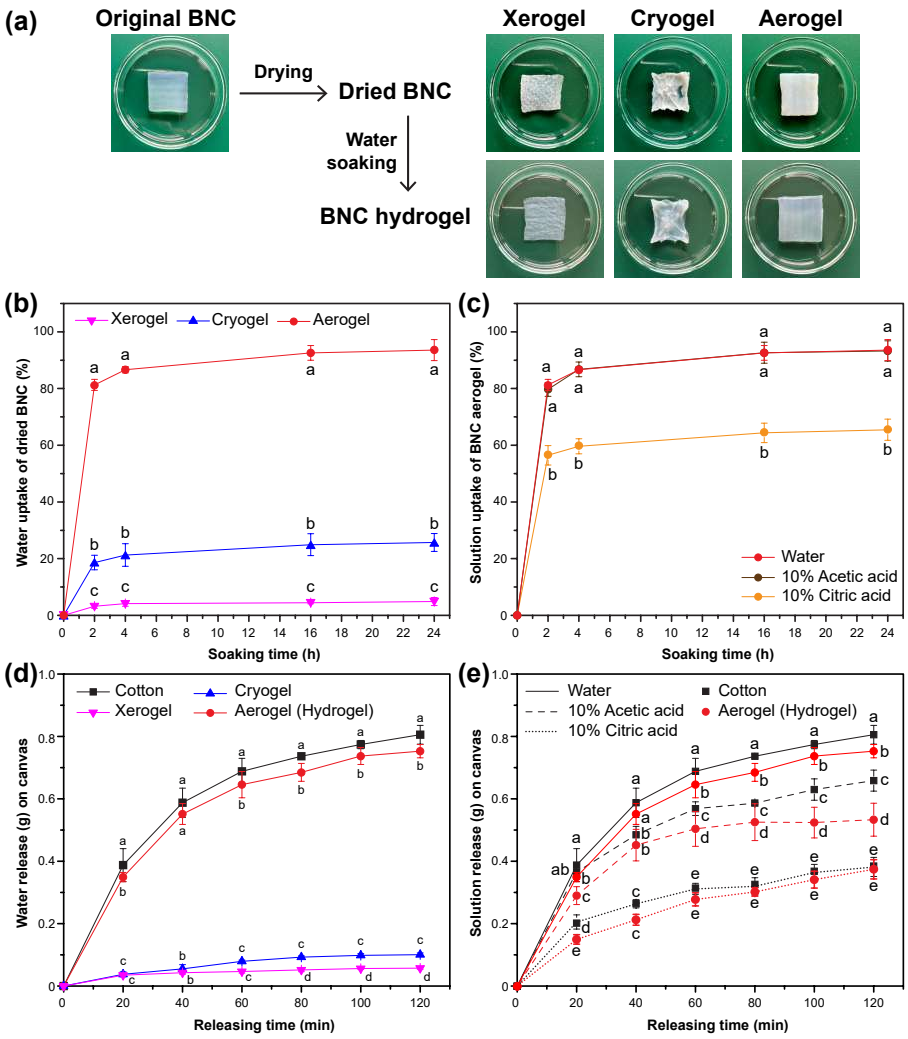

Fig. 3 BNC characteristics: (a) physical appearances of BNCs after drying with various techniques, (b) water uptake of dried BNCs, (c) solution uptake of BNC aerogel, (d) water release from BNCs and cotton pad, and (e) solution release from BNC hydrogel and cotton pad.

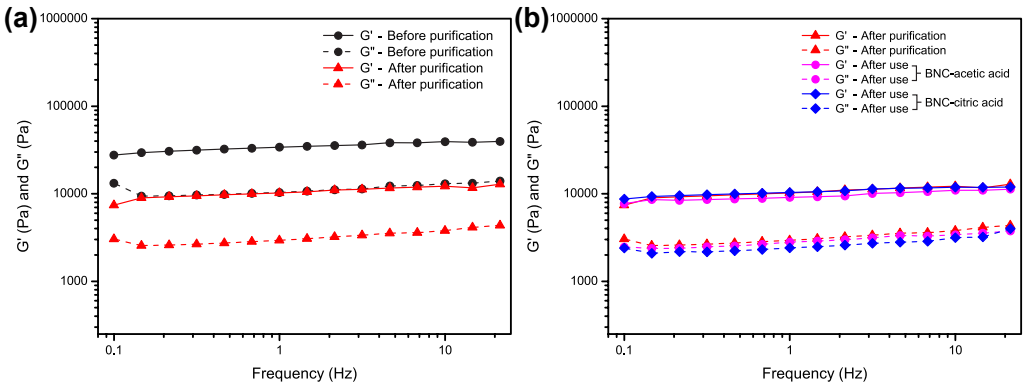

Fig. 4 Mechanical properties of hydrogels: (a) BNCs before and after purification and (b) fresh BNC after purification and used BNCs with 10% acetic acid or citric acid solutions.

exhibited noticeably lower water-release amounts than the aerogel sample, most likely due to their limited water uptake capacity. Both hydrogels from the xerogel and cryogel released most of their water within the first 20 min, after which no significant increase was observed. In contrast, the hydrogel from the aerogel showed a continuous release that increased gradually over time, and its release level was slightly lower than that of the cotton pad. The observed effect arises from the extensive porosity of the BNC's three-dimensional network and the presence of abundant free hydroxyl groups, which hold water within the nanoporous structure via hydrogen bonding. In a previously reported paper conservation context, BNC hydrogels also showed an intermediate water-release profile between cotton-based systems and agarose matrices under similar experimental trends, with cotton pad exhibiting a higher release magnitude (3.12-fold relative to BNC), while agarose showed a lower response (0.43-fold relative to BNC) [18].

In addition, this work investigated the liquid-loading and release kinetics of BNC aerogels, in which the dry aerogels were loaded with different liquids, including water, 10% v/v acetic acid, and 10% w/v citric acid, to form hydrogels. As shown in Fig. 3c, water and acetic acid solution exhibited similar uptake behavior, whereas citric acid solution showed slower uptake throughout the soaking period of 24 h. The release behavior was further examined gravimetrically on canvas by measuring the weight of solution released from cotton pads and BNC hydrogels after loading with the same weight of solution. As shown in Fig. 3e, cotton pads released all solutions more rapidly and in greater amounts than the corresponding BNC hydrogels, particularly water and acetic acid solution. In contrast, BNC hydrogels loaded with citric acid solution showed a slower and more gradual release profile, which is desirable for safe stain removal in conservation cleaning. This behavior may be mainly associated with the bulkier molecular structure of citric acid and its polar functional groups, including three carboxylic acid groups and one hydroxyl group, which could enhance interactions with the hydroxyl-rich BNC nanofiber network through hydrogen bonding. Such mechanism is consistent with previous reports showing that the BNC network can retain active compounds through physical entrapment and secondary bonding, thereby moderating their release [23]. These interactions may reduce the diffusion speed within the aerogel structure and promote longer retention of citric acid solution in the BNC hydrogels.

Mechanical properties of BNC

Viscoelasticity is a critical material property that influences the cleaning performance of hydrogel polymers. This characteristic can be assessed using a cone-plate rheometer, where the gel is subjected to controlled shear stress (Pa) over a range of oscillation frequencies (Hz). The response to external forces is depicted through frequency sweep curves consisting of the storage modulus (G'), which reflects the elastic component, and the loss modulus (G''), which corresponds to the viscous component. When G' exceeds G'', the gel behaves predominantly elastically, indicating that it can regain its shape after the external force is removed. Moreover, a greater divergence between G' and G'' (when $G' > G''$) signifies a more pronounced elastic nature. For gels intended for artwork cleaning, viscoelastic behavior is essential not only for effective removal of dirt, aged binders, or aged adhesives, but also for handling and application. The gel must retain its form on the treated area without sagging or flowing due to gravity, which is especially important for vertical paintings. In addition, it must be removable in one piece without leaving residues, and it should recover its form after use. During practical use, conservators often lift the gel using tweezers, applying a moderate level of force. Nonetheless, excessive stiffness is undesirable. A gel with moderate to low stiffness allows intimate contact with irregular and textured artwork surfaces, ensuring effective cleaning action. Consequently, an appropriate G' values for cleaning applications lies within an intermediate range of approximately 1,000–10,000 Pa [2]. Values that are too low are unsuitable; for instance, previous research reported that PVA gels with G' values between 100 and 370 Pa could not be peeled from surfaces [24].

The G' and G'' values of the raw BNC prior to purification (Fig. 4a) were above 10,000 Pa across all applied frequencies, indicating high stiffness that may render it unsuitable for use as a cleaning gel. In contrast, the purified BNC exhibited substantially lower G' and G'' values, remaining below 10,000 Pa throughout the frequency range. This reduction confirms that bacterial residues and other impurities were removed during purification and replaced by water molecules. As a result, the hydroxyl groups on the CNF became more exposed, enabling the formation of secondary bonds with water. In this state, the absorbed water acts as a plasticizer, enhancing the flexibility of the BNC hydrogel [25].

Since reusability is another essential requirement for cleaning gels, the retention of mechanical properties is an important factor to consider. Therefore, the viscoelastic behavior of the BNC hydrogels after use was also examined. The results for hydrogels loaded with acetic acid and citric acid solutions after being applied for PVAc removal on canvas are presented in Fig. 4b. The G' and G'' curves of the used BNC hydrogels nearly overlapped with those of the unused BNC (freshly purified samples), and the G' and G'' values across all applied frequencies showed no significant differences. This indicates that BNC aerogels, after being loaded with either acetic or citric acid solutions and used for PVAc removal, were able to retain their viscoelastic properties and could potentially be reused

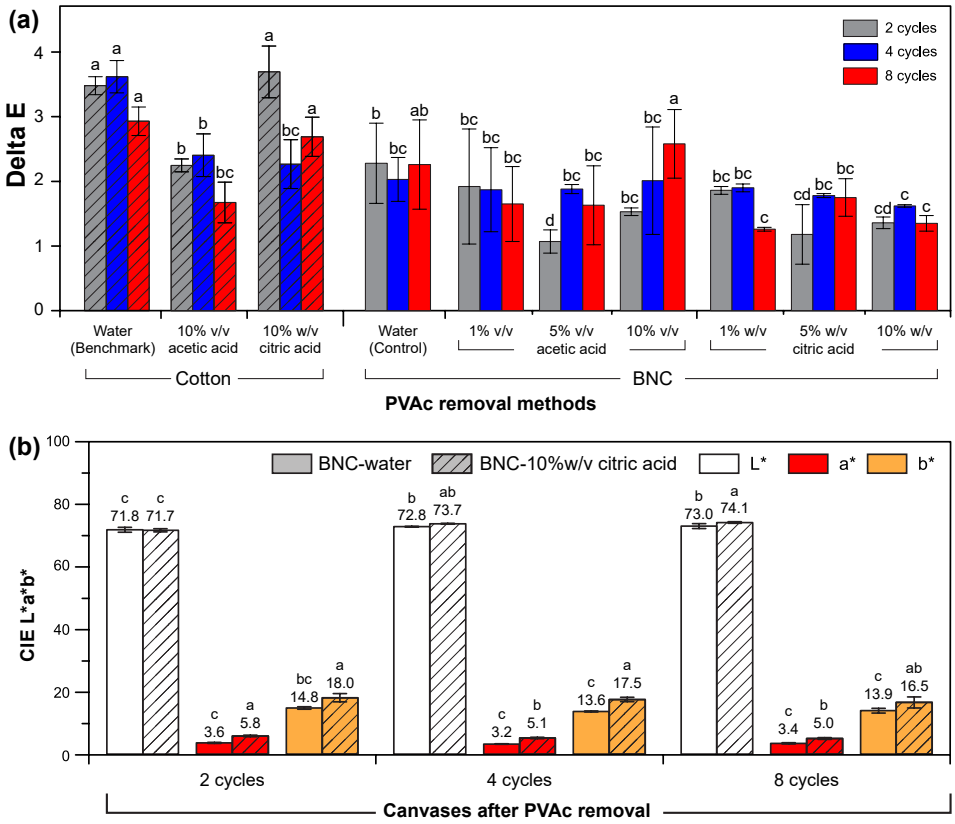

Fig. 5 Color changes of canvases after each cleaning cycle: (a) color difference between the aged PVAc-free canvas and the treated canvases and (b) color parameters of the canvases treated with water and 10% w/v citric acid for 8 cycles.

for subsequent cleaning applications.

Appearance and color of canvas before and after PVAc removal

CIE L*a*b* system consists of three parameters that describe color of sample. The L* value represents lightness, ranging from 0 to 100, where 0 corresponds to complete darkness (black) and 100 indicates maximum lightness (white). The a* value shows the position between red (+a*) and green (−a*) axis. Similarly, the b* value explains the position between yellow (+b*) and blue (−b*) axis. The examination of the color difference (delta E; ΔE) in Fig. 5a was calculated from the CIE L*a*b* values between the aged original canvas without PVAc and the treated canvas. The ΔE of less than 2 indicates that the difference cannot be visually detected by the human eye and is difficult to consider a perceivable color difference [26]. When comparing the PVAc removal methods, cotton-pad methods generally produced higher ΔE values than the BNC hydrogel methods. Although the cotton pad loaded with 10% v/v acetic acid showed relatively lower ΔE values in each cycle than those loaded with water or citric acid solution, these values do not necessarily reflect a more controlled cleaning action, as the cotton-pad approach may promote solution spreading, overcleaning, and tideline formation. An increase in the acetic acid concentration in the hydrogels resulted in higher ΔE values, and a larger standard deviation was also observed. This effect is likely attributed to acetic acid inducing mild acid hydrolysis and removing yellowed surface impurities, resulting in a brighter appearance than the original canvas. In contrast, all concentrations containing citric acid yielded ΔE values below 2, which is consistent with the visual observations at the PVAc-removed areas. Although citric acid is a triprotic acid capable of releasing three protons, its overall degree of dissociation results in a lower effective concentration of H^+ compared with acetic acid at the same molarity. Consequently, citric acid exhibited a lower tendency to cause overcleaning than acetic acid.

Fig. 5b shows the CIE L*a*b* values of the canvas treated with citric acid for PVAc removal in comparison with water treatment at each cycle. Regarding the effect of removal cycles, increasing the number of cycles resulted in different color change trends. The lightness significantly increased as the number of cycles increased. In contrast, the redness tended to decrease, particularly in the citric acid-treated canvas. However, no significant change in yellowness was observed in the canvases treated with the same solution. The observed

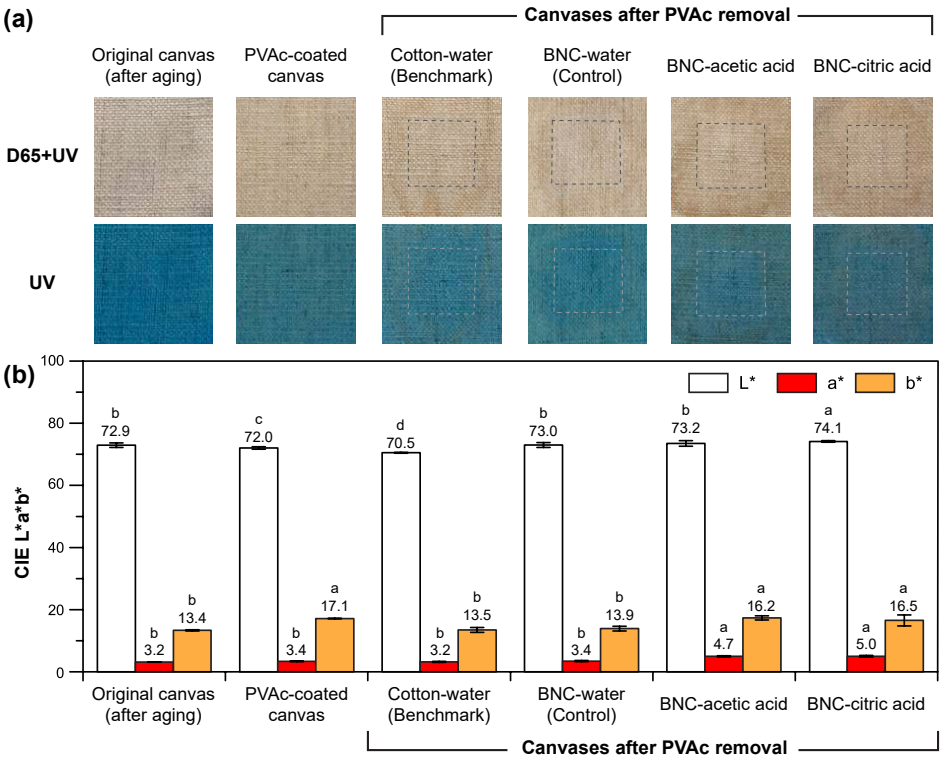

Fig. 6 Appearance and color of canvases: (a) photographs taken under different light sources, and (b) CIE L*a*b* values.

changes in CIE L*a*b* values suggest that part of the PVAc adhesive was removed from the canvas surface during treatment.

The photographs of the original canvas without PVAc after aging, as well as the canvas before and after PVAc removal using different methods (fixed at 8 cycles), are presented in Fig. 6a. For the photographs taken under the D65+UV (daylight) illumination condition, the PVAc-coated canvas exhibits a noticeably more yellowish tone compared with the original canvas. After PVAc removal, areas where the hydrogels were placed (dashed outline in Fig. 6a) appear visually distinct from the surrounding untreated areas, and the tide lines can be observed around the cleaning spots. Under UV illumination, the differences between canvases with and without PVAc become even more pronounced. The original canvas appears bluish, whereas the PVAc-coated canvas shifts toward a light green tone, indicating increased yellowing. After PVAc removal, the bluish corresponding to the hydrogel placement areas reappear. The enhanced contrast under UV light arises from the different responses of cellulose fibers in the canvas and aged PVAc to UV excitation. UV radiation promotes electronic transitions of valence electrons, and the resulting differences in fluorescence emission among molecules enhance the visual contrast. This observation is consistent with the findings of Toja et al [27], who reported that aged PVAc films containing plasticizers, after aging at 60 °C for 2 h, exhibited distinct fluorescence intensity peaks in fluorescence spectroscopy.

Conventional hydrogel systems used in conservation cleaning exhibit different limitations that influence treatment outcomes and surface appearance. Agarose gels, while widely applied for localized solvent delivery, are relatively rigid and may show limited conformability on uneven substrates, resulting in non-uniform cleaning [28]. Gellan gum systems provide tunable behavior for moisture delivery; however, their network structure is strongly influenced by the ionic environment, where cation interactions can modify gel stiffness and network organization, affecting solvent release behavior and potentially leading to variable cleaning performance and uneven moisture distribution [29]. In comparison, BNC-based hydrogels appear to offer improved conformability and more controlled solvent release through their highly porous nanofibrillar network and strong water-retention capacity, which could help promote a more uniform surface appearance after treatment [30].

According to the CIE L*a*b* values of canvases in Fig. 6b, the original canvas without PVAc exhibited a yellowish tone. After coating with PVAc and aging by heat, the canvas showed a slight yellowness, indicating an increase in yellowish tone due to the coating and the aging process. After PVAc removal, all three

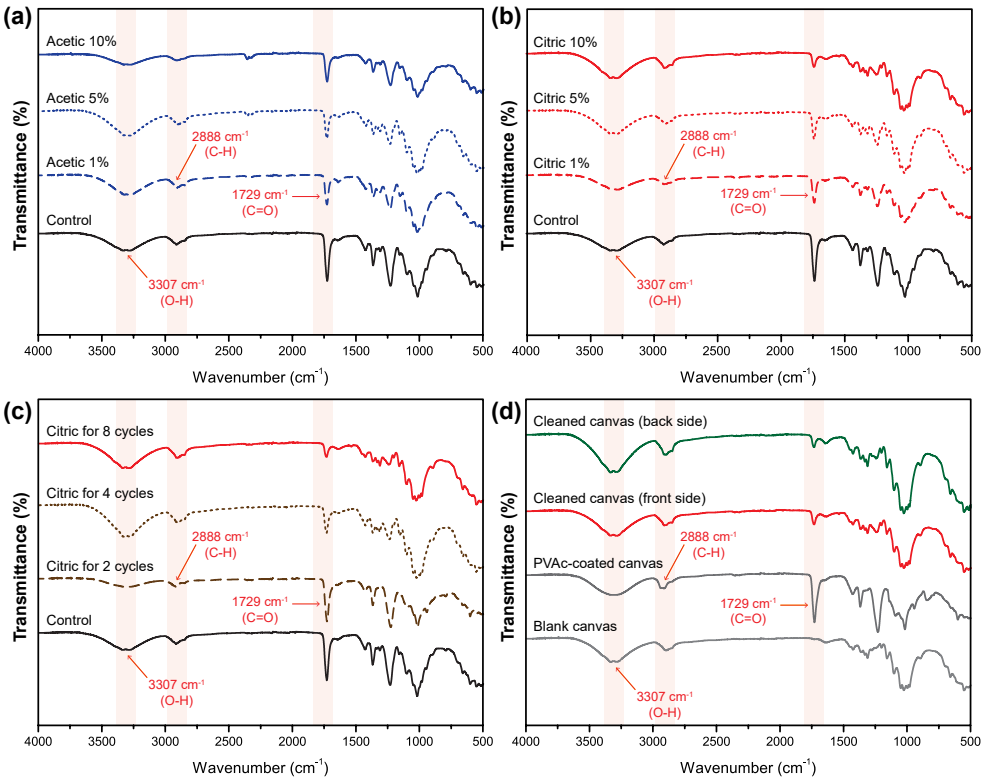

Fig. 7 FTIR spectra of treated canvas surfaces: (a) different concentrations of acetic acid solution, (b) different concentrations of citric acid solution, (c) different cleaning cycles with 10% w/v citric acid, and (d) back and front sides of the canvas (treated with 10% w/v citric acid for 8 cycles).

BNC-treated canvases exhibited significant increases lightness (L). The acid solution-treated samples also showed higher a* values, indicating increased redness, whereas the water-treated canvas exhibited reduced yellowness, as reflected by lower b* values. In conclusion, the BNC loaded with 10% citric acid achieved the most effective PVAc removal compared with the other formulations, which is consistent with the ΔE values discussed earlier.

The effective and safe removal of aged PVAc adhesive, with reduced overcleaning, by the BNC aerogel loaded with 10% citric acid was attributed to the combined chemical interaction of citric acid and the controlled-release behavior of the BNC hydrogel. Since citric acid is a hydroxy-tricarboxylic acid containing three carboxylic acid groups and one hydroxyl group, these functional groups can interact with polar groups in aged PVAc, particularly ester carbonyl groups and polar degradation products generated during ageing or partial hydrolysis [31, 32]. Such interactions could promote swelling and interfacial weakening of the aged adhesive layer, thereby reducing its adhesion to the cellulose fibers of the canvas. Moreover, the safer performance of citric acid was likely related to its larger hydroxy-tricarboxylic structure, which could be retained longer in the hydroxyl-rich nanofiber network of the BNC and promote a more gradual and localized release than the smaller acetic acid molecule, thereby lowering the tendency for overcleaning while still assisting PVAc softening and removal under mild suction applied from beneath the canvas.

Chemical structure of canvas before and after PVAc removal

The functional groups of the canvas surface before and after PVAc removal were analyzed using the FTIR technique (Fig. 7). All samples exhibited broad peaks corresponding to O—H and C—H stretching vibrations at 3307 and 2888 cm^{-1}, respectively, which are the main characteristics of cellulose [33, 34], as linen fibers are composed primarily of cellulose (approximately 70–85%). By comparison, the PVAc-coated canvas displayed a sharp peak at 1729 cm^{-1} (Fig. 7d), representing the C=O functional group attributed to the PVAc chemical structure [35].

When comparing the types of solutions used for PVAc removal on the canvas (Fig. 7a and Fig. 7b), both acetic acid and citric acid exhibited lower peak intensities at 1729 cm^{-1} than water (the control hydrogel sample), with citric acid showing a lower peak intensity than acetic acid at identical solution concentrations. The peak intensity reflects the residual

amount of PVAc remaining on the surface; therefore, the lower intensity observed in the citric acid-treated samples indicates that citric acid was more effective in dissolving PVAc than acetic acid. With regard to solution concentration, increasing the citric acid concentration led to a further decrease in the peak intensity at 1729 cm^{-1}, whereas variations in acetic acid concentration did not result in a significant change in PVAc removal efficacy.

There are two key factors governing the dissolution of PVAc: the solubility parameter and molecular interactions, particularly hydrogen bonding. The polarity difference between citric acid and acetic acid is relatively small; therefore, polarity alone has only a minor influence on PVAc dissolution. A more relevant factor is the solubility parameter (δ). PVAc has a solubility parameter of 19.4 $MPa^{1/2}$, and solvents or aqueous solutions with δ values closer to this range generally exhibit greater ability to dissolve PVAc. Citric acid possesses a higher Hildebrand solubility parameter and a stronger hydrogen-bonding capacity than acetic acid, owing to its three carboxyl groups and one hydroxyl group [36]. These features allow citric acid solutions to interact more effectively with the ester groups of PVAc, promoting polymer chain relaxation and partial hydrolysis. This characteristic results in lower carbonyl peak intensities in the FTIR spectra of citric acid-treated samples compared with acetic acid-treated samples.

However, the DI water-loaded BNC hydrogel also reduced the PVAc carbonyl signal to some extent. According to the ΔE values shown in Fig. 5a, the DI water-loaded BNC hydrogel produced a smaller color difference than the water-loaded cotton pad and showed relatively comparable ΔE values to some acid-loaded BNC hydrogels. This effect was likely attributed to the physical hydration provided by the BNC nanofiber network and the assistance of the suction-based cleaning approach. Compared with the cotton pad, the BNC hydrogel can retain water more effectively within its hydroxyl-rich nanofibrillar network and release it in a more controlled manner, especially under mild suction. This controlled water release could hydrate the linen fibers, swell or plasticize water-accessible regions of the aged adhesive, and weaken the adhesive-fiber interface. Under mild suction applied from beneath the canvas, the hydrated and loosened PVAc residues could then be partially detached from the canvas structure. Although the water-loaded BNC hydrogel produced a measurable cleaning effect and acceptable visual appearance, the lower residual carbonyl intensity observed in the acid-treated samples (Fig. 7a,b) indicates that acid loading further assisted PVAc removal beyond the physical hydration-suction process through the chemical interactions described earlier. In terms of application duration (Fig. 7c), the peak intensity was found to decrease with increasing contact time. A longer interaction period between the BNC hydrogel (loaded with 10% citric acid) and the canvas allowed more effective chemical interactions, thereby improving PVAc removal from the canvas. The C=O peak of the treated sample at 80 min showed the lowest intensity, confirming its effectiveness in dissolving PVAc. Fig. 7d compares the FTIR spectra of the treated canvas (front and back sides) with the original canvas without PVAc, showing a modest C=O peak in the treated samples. This indicates the presence of residual PVAc in the canvas, implying that extended cleaning time may be necessary to achieve complete removal. The treated front and back sides of the canvas exhibited no significant difference in carbonyl peak intensity, demonstrating that the proposed BNC hydrogel-vacuum method is effective in removing PVAc from both sides of the canvas.

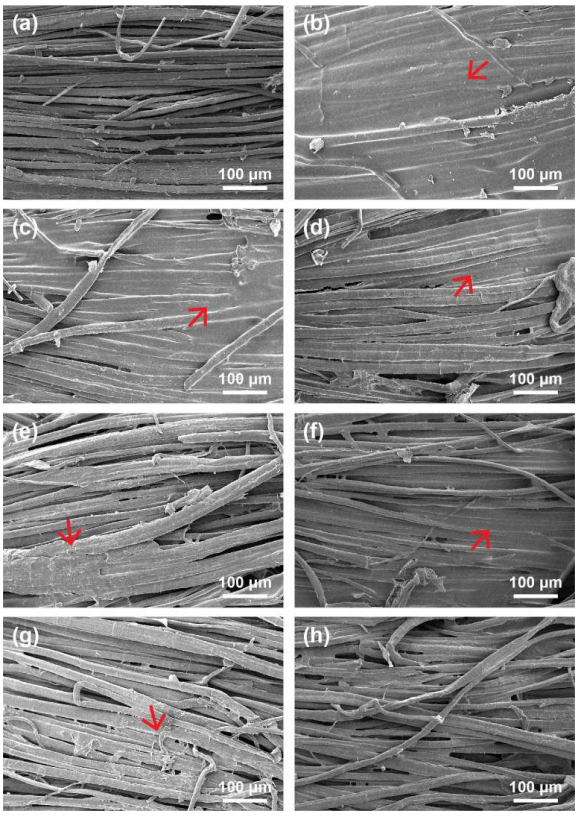

Fig. 8 SEM images of aged canvas surfaces: (a) original canvas without PVAc, (b) PVAc-coated canvas, and after PVAc removal: (c) benchmark, (d) control, (e) BNC-5% acetic acid, (f) BNC-10% acetic acid, (g) BNC-5% citric acid, and (h) BNC-10% citric acid. Red arrows indicate regions where fibers were bonded together by PVAc.

Morphology of canvas before and after PVAc removal

SEM was used to investigate the morphology of canvases after PVAc removal in comparison with the origi-

nal canvas without PVAc, as shown in Fig. 8. Fig. 8a presents the original canvas without PVAc, in which individual fibers and gaps between them can be clearly observed. When the canvas was coated with PVAc latex, the liquid latex penetrated into the fiber gaps and bound the fibers together, forming a dried PVAc film (red arrow), as illustrated in Fig. 8b. After the PVAc-coated canvas was treated using different removal methods, it was found that the benchmark, control, and BNC loaded with acetic acid samples still exhibited clusters of fibers adhered together by residual PVAc (red arrow), and a noticeably less porous structure was observed. In contrast, the canvas treated with BNC loaded with 10% w/v citric acid (Fig. 8h) showed more separated fibers and a porous structure generated by the reappearance of gaps between fibers, similar to the original canvas without PVAc (Fig. 8a). These observations indicate that citric acid-loaded BNC hydrogel exhibits superior ability to dissolve PVAc compared with acetic acid and the conventional method (the control sample).

CONCLUSION

From the performance evaluation of BNC hydrogels produced using various drying techniques, it was found that supercritical CO_2 drying effectively transformed the BNC hydrogel into an aerogel with a well-preserved nanoporous structure. This aerogel exhibited the best recovery of hydrogel characteristics after rehydration and was highly suitable for loading water-based cleaning solutions. The BNC aerogel loaded with 10% w/v citric acid and applied in eight cleaning cycles provided the most effective removal of PVAc from canvas. It produced a color difference of less than 2 between the treated canvas and the original canvas without PVAc. Additionally, FTIR analysis showed the lowest residual carbonyl peak at 1729 cm^{-1}, while SEM images revealed more individualized fibers and a reopened porous structure resembling that of the original canvas. In contrast, the use of a 10% v/v acetic acid solution resulted in overcleaning, which is undesirable in artwork conservation. After the cleaning process, the BNC hydrogel retained its mechanical properties, indicating its potential for reuse. Overall, these findings demonstrate the potential of BNC aerogel as a solution carrier for canvas cleaning, with promising applicability to other types of artwork substrates.

Acknowledgements: This work was funded by the Reinventing University Program for the fiscal year 2025, under the Global Frontier Research Development Group of the Ministry of Higher Education, Science, Research and Innovation (MHESI), Thailand, and partially supported by the Office of the Permanent Secretary (OPS), MHESI, and Thailand Science Research and Innovation (TSRI) (Grant No. RGNS 65-001). The authors would like to acknowledge the support from the 'Workshop Seminar on Painting Conservation Project Phase II' at Silpakorn University and the Department of Imaging and Printing Technology, Faculty of Science, Chulalongkorn University.

REFERENCES

1. Khaksar-Baghan N, Koochakzaei A, Hamzavi Y (2024) An overview of gel-based cleaning approaches for art conservation. *Heritage Sci* **12**, 248.
2. Leksomboon W, Aht-Ong D, Katemake P, Pacaphol K (2025) Optimizing PVA hydrogel characteristics and properties through physical and chemical crosslinking for oil-painting restoration. *Int J Polym Anal Charact* **30**, 531–542.
3. Wang J, Xu Y, Tian C, Yu Y, Zou C (2024) Application of polyvinyl alcohol–ethylene glycol hydrogel technology for removing animal glue in book restoration based on fluorescent labeling evaluation. *Nanomaterials* **14**, 1878.
4. Dan S, Xiaoying L, Xing Z, Ni X, Shasha X, Hongyi Q, Yalin L (2026) Preparation and swelling performance of green algae polysaccharide-intelligent hydrogel. *ScienceAsia* **51**, 2026007.
5. Baglioni M, Poggi G, Chelazzi D, Baglioni P (2021) Advanced materials in cultural heritage conservation. *Molecules* **26**, 3967.
6. Petrella G, Mazzuca C, Micheli L, Cervelli E, Fazio D, Iannuccelli S, Sotgiu S, Palleschi G, et al (2016) A new sustainable and innovative work for paper artworks cleaning process: gellan hydrogel combined with hydrolytic enzymes. *Int J Conserv Sci* **7**, 273–280.
7. Kaniewska K, Pilecka-Pietrusińska E, Karbarz M (2023) Nanocomposite organogel for art conservation—a novel wax resin removal system. *ACS Appl Mater Interfaces* **15**, 24798–24811.
8. Al-Emam E, Motawea A, Janssens K, Caen J (2019) Evaluation of polyvinyl alcohol–borax/agarose (PVA-B/AG) blend hydrogels for removal of deteriorated consolidants from ancient Egyptian wall paintings. *Heritage Sci* **7**, 22.
9. Al-Emam E, Soenen H, Caen J, Janssens K (2020) Characterization of polyvinyl alcohol-borax/agarose (PVA-B/AG) double network hydrogel utilized for the cleaning of works of art. *Heritage Sci* **8**, 106.
10. Abbasi Moud A (2022) Advanced cellulose nanocrystals (CNC) and cellulose nanofibrils (CNF) aerogels: bottom-up assembly perspective for production of adsorbents. *Int J Biol Macromol* **222**, 1–29.
11. Zhu W, Zhang Y, Wang X, Wu Y, Han M, You J, Jia C, Kim J (2022) Aerogel nanoarchitectonics based on cellulose nanocrystals and nanofibers from eucalyptus pulp: preparation and comparative study. *Cellulose* **29**, 817–833.
12. Zhou Y, Reshmy R, Philip E, Thomas D, Sindhu R, Bhargava PC, Tiwari A, Ruiz HA, et al (2023) Bacterial nanocellulose: optimized synthesis and biomedical applications. *Ind Crop Prod* **205**, 117589.
13. Ahmed Abdel Hakim, Mourad R (2023) Nanocellulose and its polymer composites: preparation, characterization, and applications. *Russ Chem Rev* **92**, RCR5076.
14. Makharita RR, El-Ahmady El-Naggar N, Baghdadi AM, Hamouda RA (2025) Sustainable production of bacterial nanocellulose from date fruit waste using *Bacillus haynesii* for waste valorisation and crystal violet dye removal. *Sci Rep* **15**, 25133.

15. Pacaphol K, Katemake P, Bankeeree W, Tse N (2025) Enzyme-loaded bacterial nanocellulose aerogel as a bio-cleaning material for artwork restoration. *Sci Rep* **15**, 25536.
16. Ahmed HE, Kolisis FN (2011) An investigation into the removal of starch paste adhesives from historical textiles by using the enzyme α-amylase. *J Cult Herit* **12**, 169–179.
17. Kumar N, Sarkar BC, Sharma HK (2012) Mathematical modelling of thin layer hot air drying of carrot pomace. *J Food Sci Technol* **49**, 33–41.
18. Leksomboon W, Bankeeree W, Tse N, Pacaphol K (2026) Novel bio-cleaning approach using xylanase and bacterial nanocellulose aerogel for foxing removal in paper conservation. *J Cult Herit* **80**, 13–25.
19. Latré SK, Desplentere F, Seveno D (2018) Computational modeling of thermal phenomena in nanomaterials for building applications. *In: Reference Module in Materials Science and Materials Engineering*, pp 1–16.
20. Cao H, Duan L, Zhang Y, Cao J, Zhang K (2021) Current hydrogel advances in physicochemical and biological response-driven biomedical application diversity. *Signal Transduction Targeted Ther* **6**, 426.
21. Sadaf N, Tuhanioglu A, Hettiarachchy N, Ubeyitogullari A (2024) Effect of a novel drying method based on supercritical carbon dioxide on the physicochemical properties of sorghum proteins. *RSC Adv* **14**, 5851–5862.
22. Al Abdallah H, Tannous JH, Abu-Jdayil B (2024) Cellulose and nanocellulose aerogels, their preparation methods, and potential applications: A review. *Cellulose* **31**, 2001–2029.
23. Anuchitworawong T, Hankum T, Aht-Ong D, Seraypheap K, Pacaphol K (2026) Bacterial nanocellulose-potassium sorbate biopolymer film as functional coating for quality retention of postharvest sweet basil. *J Polym Res* **33**, 139.
24. Riedo C, Caldera F, Poli T, Chiantore O (2015) Poly(vinylalcohol)-borate hydrogels with improved features for the cleaning of cultural heritage surfaces. *Heritage Sci* **3**, 23.
25. Rebelo AR, Archer AJ, Chen X, Liu C, Yang G, Liu Y (2018) Dehydration of bacterial cellulose and the water content effects on its viscoelastic and electrochemical properties. *Sci Technol Adv Mater* **19**, 203–211.
26. Mokrzycki W, Tatol M (2011) Color difference delta E: A survey. *Mach Graph Vis* **20**, 383–411.
27. Toja F, Saviello D, Nevin A, Comelli D, Lazzari M, Levi M, Toniolo L (2012) The degradation of poly(vinyl acetate) as a material for design objects: A multi-analytical study of the effect of dibutyl phthalate plasticizer. Part 1. *Polym Degrad Stab* **97**, 2441–2448.
28. Duncan TT, Sullivan MR, Hughes AE, Morales KM, Chan EP, Berrie BH (2025) The role of adsorption in agarose gel cleaning of artworks on paper. *Gels* **11**, 965.
29. Henniges U, Brückle I, Khaliliyan H, Böhmdorfer S (2024) Gellan residues on paper: Quantification and implication for paper conservation. *Heritage Sci* **12**, 54.
30. Sonaglia E, Schifano E, Sharbaf M, Uccelletti D, Felici AC, Santarelli ML (2024) Bacterial nanocellulose hydrogel for the green cleaning of copper stains from marble. *Gels* **10**, 150.
31. Bondancia TJ, de Aguiar J, Batista G, Cruz AJG, Marconcini JM, Mattoso LHC, Farinas CS (2020) Production of nanocellulose using citric acid in a biorefinery concept: Effect of the hydrolysis reaction time and techno-economic analysis. *Ind Eng Chem Res* **59**, 11505–11516.
32. Squillace O, Fong R, Shepherd O, Hind J, Tellam J, Steinke N-J, Thompson RL (2020) Influence of PVAC/PVA hydrolysis on additive surface activity. *Polymers* **12**, 205.
33. El Sayed NAA, El-Bendary MA, Ahmed OK (2023) A sustainable approach for linen dyeing and finishing with natural lac dye through chitosan biomordanting and microwave heating. *J Eng Fibers Fabr* **18**, 15589250231155882.
34. Sophonputtanaphoca S, Prasongsuk S, Chutong P, Samathayanon C, Cha-aim K (2023) Utilization of sugarcane bagasse for synthesis of carboxymethylcellulose and its biodegradable blend films. *ScienceAsia* **49**, 541–552.
35. D'Amelia RP, Mancuso J, Nirode W (2019) The characterization of poly n-vinyl pyrrolidone-polyvinyl acetate (PVP-PVAC) copolymers and blends by nuclear magnetic resonance spectroscopy, Fourier transform infrared spectroscopy, and elemental analysis. *J Polym Biopolym Phys Chem* **7**, 1–9.
36. Książek E (2023) Citric acid: Properties, microbial production, and applications in industries. *Molecules* **29**, 22.